International Journal of Engineering and Advanced Technology Studies,14 (1),41-63,2026
Print ISSN: 2053-5783(Print)
Online ISSN: 2053-5791(online)
Website: https://www.eajournals.org/
Publication of the European Centre for Research Training and Development -UK

Mathematical Modeling of Fluidized Bed Reactor for CO_2 Capture in a Typical Cement Producing Plant Existing in Nigeria

Otie O. Nathaniel [1], A.A. Wordu[3], E.O. Ehirim[2], T.T.Gloria[3], Miebi N Lambert[4]
[1,2,3 & 4]River State University, Port Harcourt, Nigeria
Correspondent Author: otienathaniel@gmail.com

doi: https://doi.org/10.37745/ijeats.13/vol14n14163 Published May 17 2026

Citation: Nathaniel, O. O., Wordu A. A., Ehirim E. O, Gloria T. T., Lambert, Miebi N. (2026) Mathematical Modeling of Fluidized Bed Reactor for CO2 Capture in a Typical Cement Producing Plant Existing in Nigeria, International Journal of Engineering and Advanced Technology Studies,14 (1),41-63

Abstract: *Calcium looping technology has a high potential for capturing CO_2 in Typical Cement Producing Plant Existing in Nigeria Power Generation Plant. This work modelled the calcium looping process utilizing a twin fluidized bed reactor. Incorporating the technology into the plant required the carbonator to operate under a flow rate of 0.55 m^3/s and the regenerator at 0.85 m^3/s to capture 181,175 metric tonnes of CO_2 in 724,000 metric tonnes of flue gas produced from the power plant annually. The model equations developed were solved numerically using the Runge-Kutta Fourth Order method. Math Works was used to analyze the impact of performance parameters such as temperature, reactor height, residence time, and particle size. The result showed promise for capturing 81.8% of CO_2 from the flue gas in the carbonator at a temperature of 450^{o}C, and recovering 61.7% of highly concentrated CO_2 in the regenerator at a temperature 1200^{o}C and a residence time of 30 mins.*

Keywords: Kinetics, MATLAB, cement industry, capturing and sequestration (CCS), Runge-Kutta approach; calcium looping process, greenhouse gases (GHGs), fossil fuel

INTRODUCTION

Fossil fuels which are known as mixtures of hydrocarbons recovered on daily bases from conventional and unconventional reservoirs (Igwe *et al.,* 2026; Sammy *et al.,* 2023; Ugi *et al.,* 2023; Ogolo *et al.,* 2026) though serves as vital material for energy and trade but still promotes greenhouse gases (GHGs) emission when combusted, of which carbon dioxide (CO_2) is one of the most emitted. Crude oil consumption isn't the only source of carbon dioxide (CO_2) emission, coal consumption and some other industrial processes that are in most time not regarded as foots of carbon emission such as the cement producing plants also have great amounts of carbon dioxide emitted on daily bases which has the potency of destroying or endangering the ecosystem. Within the year 2022, the cement industry such as that within countries like Nigeria were rated to contribute over 1.7 million metric tonnes of CO_2, of which currently the value tends to keep increasing as the production rate of cements has tends to increase proportionally to increase in

developments and population. Carbon dioxide in our environments promotes the impacts of greenhouse gases to man, which includes acidic rain formation, promotion of metallic corrosion which is known to be very destructive to machines / metallic materials lifespan and durability (Ugi *et al.,* 2023; Benedict and Fredrick, 2023, Benedict *et al.,* 2022; Ugi *et al.,* 2023; Ugi *et al.,* 2026; Ugi *et al.,* 2021) alteration of air sanity, increases thermal pollution, etc (Ugi *et al.,* 2023; Perry's and Green, 2007; Octave, 1999; Wordu *et al.,* 2023) which intern affect a lot of things including food availability, hence reduces the feeding nature of a country (Modestus *et al.,* 2025). Carbon dioxide presence in our today's environment is obtained from either the natural source or anthropogenic, of which Natural sources accounts for the majority of CO_2 released into the atmosphere. Animal and plant respiration, decomposition of organic matter or biowaste, forest fires, and emissions from volcanic eruptions are some of the well-known natural sources of which CO_2 is been generated into the environment (Ugi *et al.,* 2023; Ugi *et al.,* 2025). Anthropogenic sources of CO_2 are part our everyday activities and include those from power generation, transportation, industrial sources, chemical production, petroleum production, and agricultural practices. Many of these source types burn fossil fuels (such as coal, oil and natural gas), with CO_2 emissions as by product, and among all, the power generation plants contribute the greatest amount of anthropogenic CO_2 to the atmosphere (Perry's and Green, 2007).

Industrialization, population and growth in technological wellbeing of a country are the major categories that facilitates CO_2 concentration at the environment, and for this reasons countries such as China and the United States are rated the highest CO_2 emission bodies in the world with over 11.47 and 5.01 billion metric tonnes CO_2 generated in 2021, respectively (Tiseo, 2023).

Carbon dioxide in the environment has a lot to do to man, even including the promotion of cancerous cells formation with other deadly health illnesses which keeps facilitating mortality rate on a daily bases, and for these reasons, a need to reduce the CO_2 in the environment calls for different researchers' contributions on a daily bases globally. Capturing and sequestration of carbon dioxide from the environment has proven to be one of the most essential concept that protects man's environments and makes industrialization eco-friendly when effectively applied in the industrial system (Ugi *et al.,* 2023; Jorhm, 2005; Perry's and Green, 2007; Sammy *et al.,* 2023), and this carbon capturing and sequestration (CCS) processes are of diverse forms, and differs in their mode of applications and potency. Several different technologies can be used to capture CO_2 at a power plant or industrial facility. They fall into three categories: post-combustion carbon capture, pre-combustion carbon capture and oxy-fuel combustion systems (Gonzales *et al.,* 2020).

Post-combustion Carbon Capture Technology

Post-combustion capture (PCC) is useful for separating CO_2 from exhaust gases created by burning fossil fuel. PCC is an energy intensive and expensive process that is the subject of considerable research using

a variety of technologies, including solvents, sorbents and membranes. Membrane-based PCC exploits the differences in partial pressure across a selective membrane layer to separate CO_2 from other components (Basile *et al.* 2011). Sorbent-based PCC uses a sorbent material to capture CO_2 from other components by reacting with chemical reaction. This particular separation pioneered the chemical looping process. The chemical reaction produces a carbonate which is then regenerated by decomposing the carbonate to produce relatively pure CO_2 stream and regenerating the sorbent material to be used again. Solvent-based PCC employs a liquid solvent, typically amine solution. The amine selectively absorbs the CO_2 from the other components. In this process, a CO_2-rich amine is then regenerated by stripping the CO_2 out of the liquid with steam, allowing the lean amine to be recycled to the absorber while producing concentrated CO_2 stream (Jongpitisub *et al.,* 2015).

Pre-combustion Carbon Capture Technology

Pre-combustion capture involves the removal of CO_2 prior to combustion. The capture process consists of three stages (Basile *et al.* 2011):

i. The hydrocarbon fuel (typically methane or gasified coal) is converted into hydrogen and carbon monoxide (CO) to form a synthesis gas;
ii. CO is converted into CO_2 by water gas shift reaction;
iii. CO_2 is separated from hydrogen, which could be combusted cleaning. The CO_2 can be compressed into liquid and transported to a storage site.

The benefits of this process are: verified industrial scale technology in oil refineries, 90 – 95% of CO_2 emissions capture and it can produce H_2 as a transportable energy carrier or liquid fuels from coal. Nevertheless, pre-combustion capture requires high investment.

Oxy-fuel Combustion Systems

In oxy-fuel combustion capture, the fuel is combusted in the presence of nearly pure (approximately 98%) oxygen to ensure that the products of combustions contain CO_2 and water with only trace amounts of other gases (Basile *et al.* 2011). Moreover, the other significant advantage of oxy-fuel combustion is that CO_2 emissions can be almost eliminated from the exhaust. This can be achieved by recycling or separation from water vapour after condensation. As a result, nearly pure CO_2 can be compressed, but the purity of CO_2 should depend on a trade-off between efficiency losses and operational costs during purification and the safety demands of transportation and storage (Chen *et al.*, 2012).

Chemical Absorption

In is this method, the flue gas is cooled and freed from impurities. It then fed into a chemical stripping column where it comes in contact with a solvent. CO_2 in the flue gas reacts with the solvent and gets

absorbed in it. The bottom stream of the stripping column containing the rich-solvent is transferred to another column where the absorption process is reversed in the presence of heat. The lean-solvent is then recycled back to the absorber, whereas the captured CO_2 gets compressed and prepared for storage (Wong & Bioletti 2002). Chemical absorption is the most suitable method for the separation of CO_2 from exhaust gases when CO_2 has a low concentration, 5 – 15% by volume, in a gaseous stream at atmospheric pressure.

Fundamentally the are different well applied approaches of carbon capturing and reduction, but amongst, the most applied are the following:

i. Biological carbon capturing approach
ii. Carbon looping technological approach
iii. Carbon storage for enhanced oil recovery (EOR) processes

Each of these processes of CCS are applied in different countries in the world, and have been contributively acknowledged by man on daily bases, though still requires optimization measures to ensure the attainment of the global carbon concentration demand of 2050 (Ugi *et al*., 2023; Igwe *et al.*, 2026; Sammy *et al.*, 2023).

The Calcium looping or the regenerative calcium cycle, is a second-generation carbon capture technology that enables CO_2 separation from flue gases of industrial processes. It is the most developed form of carbonate looping, where a metal (M) is reversibly reacted between its carbonate form (MCO_3) and its oxide form (MO). In calcium looping process, the two species are calcium carbonate ($CaCO_3$) and calcium oxide (CaO). The captured carbon dioxide can then be transported to a storage site. Calcium looping is being developed as it is a more efficient, less toxic alternative to current post-combustion capture processes such as chemical scrubbing (Ahn *et al.*, 2013). In calcium looping process, the CaO-based sorbent, typically derived from limestone, reacts via the reversible reaction described in the reaction scheme represented below. The forward reaction, exothermic step is called carbonation while the backward step, endothermic step is called calcination and is repeatedly cycled between two vessels.

$$CaO_s + CO_2 \rightleftharpoons CaCO_{3_s} \qquad \Delta H = -178\ KJ/mol$$

Flue gas containing CO_2 is fed to the first vessel, the carbonator, where carbonation occurs. The $CaCO_3$ formed is passed to another vessel, the calciner. Calcination occurs at this stage, and the regenerated CaO is quickly passed back to the carbonator, leaving a pure CO_2 stream behind. As this cycle continues, CaO sorbent is constantly replaced by fresh reactive sorbent (Blamey *et al.*, 2010). The highly concentrated CO_2 from the calciner is suitable for sequestration, and the spent CaO has potential uses in the cement industry. The necessary heat for calcination can be provided by oxy-combustion of coal. Oxy-combustion of coal is a pre-combustion capture technology. In this process, pure oxygen rather than air s used for combustion, eliminating the large amount of nitrogen in flue gas stream. After, particulate matter is

removed, the flue gas consists only of water, CO_2 and trace amounts of other pollutants. The flue gas stream is then compressed to remove water vapor and additional removal of air pollutants, a nearly pure CO_2 stream suitable for storage is produced.

Fluidized bed reactors are found in a large number of applications in the environmental, chemical and process industries (Winter & Schratzer, 2013) and can also be potentially considered for calcium looping process. In fact, the calcium looping process in its application for CO_2 capture was originally conceived by means of twin fluidized bed reactors (Shimizu *et al.,* 1999). Most of the already pilot plants for CO_2 capture are based on fluidized bed reactors (Hanak *et al.,* 2015) and a large number of models can be found in literature (Lasheras *et al.,* 2011; Romano, 2012; Ylätalo *et al.,* 2012; Lisbona *et al.,* 2013). fluidized bed reactors are widely employed as they provide large gas-solid contact surface, which promotes heat and mass transfer. The fluidized-bed reactor has the ability to process large volumes of fluid.

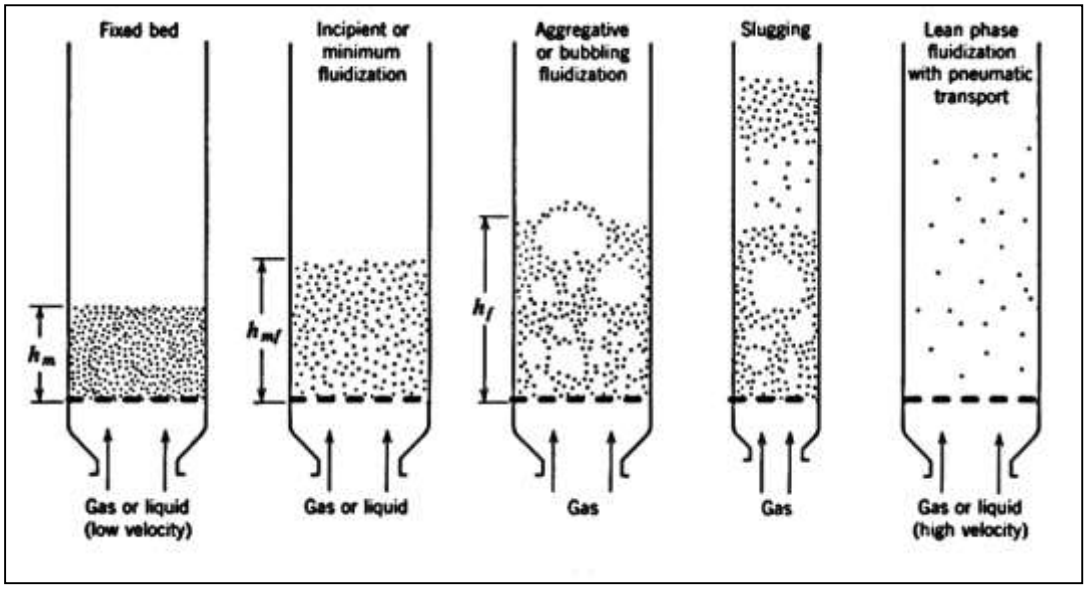

Fig. 1: Different kinds of contacting of a batch of solids by fluid. (Kunni & Levenspiel, 1977)

Fluidization occurs when small solid particles are suspended in an upward flowing stream of fluid. The fluid velocity is sufficient to suspend the particles, but it is not large enough to carry them out of the vessel. The solid particles swirl around the bed rapidly, creating excellent mixing among them (Figure 1). The material "fluidized" is almost always a solid and the "fluidizing medium" is either a liquid or gas. The characteristics and behavior of a fluidized bed are strongly dependent on both the solid and liquid or gas properties. Nearly all the significant commercial applications of fluidized-bed technology concern gas-solid systems.

At low gas velocities, the solid particles experience drag from the flowing gas, and the pressure drop caused by this drag adheres to the Ergun equation, similar to other packed bed systems. However, as the gas velocity rises to a specific threshold, the cumulative drag acting on the particles matches the weight of the bed. At this point, the particles will commence lifting and enter a state of minimal fluidization. If ρ_c represents the density of the solid catalyst particles, A_c denotes the cross-sectional area, h_s indicates the height of the bed settled before particle lift-off begins, h signifies the height of the bed at any given moment, and ε_s and ε represent the respective porosities of the settled and expanded bed, then the mass of solids within the bed, denoted as W_s, can be expressed as:

$$W_s = \rho_c A_c h_s(1 - \varepsilon_s) = \rho_c A_c h(1 - \varepsilon) \qquad \text{(i)}$$

This relationship arises due to the constancy of the mass of the bed occupied exclusively by the solid particles, irrespective of the bed's porosity. When the drag force surpasses the gravitational force, the particles commence lifting, leading to an expansion of the bed, which results in an increase in bed porosity. This increase in bed porosity decreases the overall drag until it is again balanced by the total gravitational force exerted on the solid particles (Incipient or minimum fluidization). As the gas velocity is further increased, the bed expansion continues. Solid particles begin to separate and start moving in a restless manner, sometimes jostling against each other. A slight increase in velocity leads to instabilities, causing some of the gas to bypass the rest of the bed in the form of bubbles (Aggregative or bubbling fluidization). These bubbles grow in size as they ascend the column. Concurrently, the solids within the bed start moving vigorously in an upward, downward, and swirling fashion, resembling a boiling, frothing mixture. With gas bubbling through the bed and the solid particles behaving like part of the fluid, the bed of particles is considered to be in a "fluidized" state. This state is characterized by aggregative, nonparticulate, or bubbling fluidization.

As the gas velocity is further increased, slug flow (as depicted in Slugging) and unstable, chaotic bed operation can occur. Eventually, at extremely high velocities, the solid particles can be blown or transported out of the bed (as shown in lean phase fluidization with pneumatic transport). The range of velocities over which the Ergun equation remains applicable can be quite extensive. However, the difference between the velocity at which bed expansion begins and the velocity at which bubbles start to appear can be extremely small, sometimes even nonexistent. This observation implies that when steadily increasing the gas flow rate, the initial sign of bed expansion might be the emergence of gas bubbles in the bed and the movement of solid particles. At low gas velocities within the fluidization range, the rising bubbles contain very few solid particles. The remaining portion of the bed has a much higher concentration of solids and is referred to as the emulsion phase of the fluidized bed. The bubbles are termed the bubble phase, and the cloud phase represents an intermediate phase between the bubble and emulsion phases.

Some researchers have dived into assessment of fluidized bed reactor in CO_2 capturing, and with different vies proved the abilities of the system been able to reduce CO_2 from streams of fluids. Fang *et al.* (2009) conducted experimental investigations into the capture of CO_2 from flue gases using a small fluidized bed reactor with limestone as the sorbent material. The findings revealed that limestone exhibited a high level of efficiency in capturing CO_2 from flue gases. However, as the number of carbonation/calcination cycles increased, the CO_2 capture capacity of limestone gradually decreased. Practically, in some scenarios, coal might be needed to supply the heat required for $CaCO_3$ calcination. This could potentially affect the sorbent's capacity for CO_2 capture. Experimental results demonstrated that the variation in CO_2 capture capacity when using a mixture of limestone and coal ash, in relation to the number of cycles, exhibited a qualitative similarity to the variation observed when using limestone alone. Moreover, the study showed that the cyclic stability of limestone, whether it underwent the kinetically controlled stage in the carbonation process alone or both the kinetically controlled stage and the product layer diffusion-controlled stage, had negligible differences. Based on the experimental data, the researchers developed a model for a high-velocity fluidized bed carbonator, comprising a dense bed zone and a riser zone. This model predicted that the high-velocity fluidized bed carbonator, when incorporated into a continuous carbonation and calcination system and operated under reasonable conditions, could achieve CO_2 capture efficiencies exceeding 80%.

Zhao and Zhang (2020) emphasized the significance of CaO-based absorbents as highly effective materials for high-temperature CO_2 capture. Nevertheless, a critical issue emerged with extended usage: the gradual decline in CO_2 absorption performance over multiple cycles. This decline necessitated the constant replenishment of fresh absorbent, leading to substantial increases in both economic costs and equipment loads. Consequently, there was a pressing need to reduce the raw material costs associated with CaO-based absorbents while simultaneously preserving their high-cycle absorption efficiency and stability through modification. The study initially analyzed the principles of decarburization in CaO-based absorbents and delved into the factors responsible for the deterioration of absorption performance. Subsequently, the research summarized the primary modification methods and their respective effects on CaO-based absorbents, prepared using different calcium sources such as natural minerals, chemical agents, and bulk industrial solid waste. These modifications aimed to enhance absorption efficiency, improve cycling stability, and reduce overall costs. The results of the investigation highlighted that CaO-based absorbents crafted from industrial solid waste possessing a high calcium content demonstrated excellent CO_2 absorption efficiency and cycle stability. Additionally, a modest presence of impurities in the solid waste was found to enhance the corrosion resistance and wear resistance of CaO-based absorbents. Furthermore, the study emphasized the potential for minimizing the production cost of CaO-based absorbents through integration with industrial production processes, providing a promising avenue for cost-effective CO_2 capture solutions.

Arias *et al.* (2020) conducted a research project focusing on the thermal integration of a flexible calcium looping CO_2 capture system within an existing coal power plant designed for backup purposes. This investigation centered on CO_2 capture methodologies applied to backup power plants, employing calcium looping systems in conjunction with substantial quantities of Ca-solids. The key innovation of this study was the incorporation of an adaptable CO_2 capture system into an established power plant, which was based on a previously documented concept. This integrated system featured a compact oxy-fired calciner, accounting for just 8% of the total thermal capacity, dedicated to the continuous regeneration of sorbents. Additionally, a carbonator reactor was introduced to capture 90% of the emitted CO_2 as $CaCO_3$, following the operational cycles of the backup power plant. Notably, significant stockpiles of rich CaO and $CaCO_3$ solids were maintained at moderate temperatures for efficient utilization. During the operation of the backup plant, calcined solids were brought into contact with flue gases within the carbonator reactor, while the oxy-calciner maintained continuous operation in a steady state. In order to enhance the flexibility of the CO_2 capture system and mitigate the associated cost escalation stemming from additional equipment necessary solely during brief backup periods, a proposal was formulated.

This proposal aimed at harnessing the steam cycle of the existing power plant to recuperate a substantial portion of the heat from the streams exiting the carbonator. This approach enabled the preservation of electrical power output while simultaneously reducing the thermal input to the power plant by 12%, thereby reducing the size of the associated CO_2 capture equipment. To satisfy the auxiliary power requirements for the oxy-calciner block, a compact steam cycle was devised, capitalizing on the waste heat derived from streams exiting this reactor. Through meticulous resolution of mass and heat balances and the presentation of a viable thermal integration scheme utilizing Aspen Hysys, it was ascertained that CO_2 emissions originating from well-amortized power plants, when employed as backups, could be captured with a net efficiency of 28%.

Scaltsoyiannes and Lemonidou (2020) explored the versatile applications of calcium looping in various environmental contexts, including post-combustion CO_2 capture, sorption-enhanced reforming, and thermochemical energy storage. However, they noted that certain aspects of the calcination reaction mechanism and the influence of CO_2 partial pressure remained insufficiently understood, prompting a need for further investigation. This study primarily focused on the kinetic modeling of the calcination reaction. To delve into the kinetics of limestone calcination, the researchers conducted experimental studies in a fixed-bed reactor. They also employed various models previously documented in the literature to provide theoretical insights. Among these models, the Uniform Conversion Model (UCM) and the Changing Grain Model (CGM) demonstrated superior performance in describing the conversion-time data compared to the Random Pore Model (RPM). Furthermore, the study introduced a Langmuir-Hinshelwood mechanistic model, which encompassed key aspects such as the decomposition of $CaCO_3$, the desorption of CO_2, and the relaxation of CaO*. This mechanistic model yielded a close fit to the

observed reaction rate values and allowed for the determination of an activation energy of 210 kJ/mol and a pre-exponential factor of 18,860 kmol/(m^2s). Crucially, the proposed model's validity was confirmed through its ability to accurately predict decomposition rates reported by other researchers under diverse conditions, enhancing our understanding of the calcination kinetics of limestone.

Maparanyanga and Lokhat (2021) employed a simulation approach to model the Calcium-looping process. They utilized one-dimensional mass and energy balance equations to describe the behavior of interconnected fluidized bed reactors within the system. Kinetic parameters for both the carbonator and calciner reactions were initially drawn from existing literature sources and subsequently refined to account for the influence of sulphation. To evaluate the efficiency of the process, the researchers conducted a series of sensitivity analyses, comparing the apparent degree of carbonation with the actual level of carbon dioxide removal. Their findings revealed a noteworthy trend: as temperature increased, the degree of carbonation decreased, while sulphation exhibited an opposite behavior by increasing with rising temperatures. Furthermore, the study observed that the activity of calcium oxide decreased as the number of carbonation-calcination cycles increased. A crucial conclusion drawn from this research was the significance of considering the impact of sulphation in the design of calcium-looping systems. Neglecting this effect could lead to an overestimation of the number of active calcium particles available to react with carbon dioxide, which has important implications for the system's performance and efficiency.

Past efforts have primarily concentrated on employing the continuous twin fluidized bed calcium looping process for CO_2 capture. Furthermore, it fails to provide sufficient duration for the CaO-based sorbent to interact with CO_2 within the carbonator or for $CaCO_3$ to undergo thermal decomposition in the regenerator, resulting in the production of low yield of concentrated CO_2 and CaO. In contrast, a batch-wise system offers an extended residence time for the sorbent to react with CO_2, resulting in increased CO_2 capture. The present research endeavors to investigate a batch-wise calcium looping system, wherein the carbonator is situated within the plant, while the regenerator or calciner is located offsite.

MATERIALS AND METHODS

Materials used for the Study

To attain correct modeling bases over the dynamic study of the system, computer programs are linked to the work to assist in the accurate evaluation of the system dynamically. Some of the materials used are;

i. Computer
ii. MATLAB Program language
iii. Chemical Engineering Handbooks

Performance Modeling of the Studied System

Concentration gradient Model

Mathematical representation of the calcium-looping process for CO_2 capturing using a fluidized bed reactor is modelled in this work in consideration of the flow nature of the fluid as well as the orientation of the fluidized bed reactor

$$\text{Total inflow into Carbonator} = \dot{m}_{CaO,0} + \dot{m}_{cCO_2,in} + \dot{m}_{rCaO} \quad (1)$$

$$\text{Total outflow from Carbonator} = \dot{m}_{cCO_2,out} + \dot{m}_{cCaCO_3} \quad (2)$$

$$\text{Generation within Carbonator} = r_c \quad (3)$$

$$\frac{dm_1}{dt} = \dot{m}_{CaO,0} + \dot{m}_{cCO_2,in} + \dot{m}_{rCaO} - \left(\dot{m}_{cCO_2,out} + \dot{m}_{cCaCO_3}\right) + r_c \quad (4)$$

$$\text{Total inflow into Regenerator} = \dot{m}_{inert} + \dot{m}_{cCaCO_3} \quad (5)$$

$$\text{Total outflow from the Regenerator} = \dot{m}_{rCO_2} + \dot{m}_{rCaO} \quad (6)$$

$$\text{Generation within Regenerator} = r_r \quad (7)$$

$$\frac{dm_2}{dt} = \dot{m}_{inert} + \dot{m}_{cCaCO_3} - \left(\dot{m}_{rCO_2} + \dot{m}_{rCaO}\right) + r_r \quad (8)$$

Where, $\dot{m}_i$ is the mass flow rate of species i, m is the mass in the reactor at any time, r_c and r_r are the rate reactions for carbonation and regeneration steps respectively.

The material balance for the bubble phase can be derived as follows from the principle of conservation of mass:

$$\begin{bmatrix}\text{Rate of accumulation}\\ \text{of species i}\end{bmatrix} = \begin{bmatrix}\text{Rate of input of species}\\ \text{i into differential}\\ \text{elment}\end{bmatrix} - \begin{bmatrix}\text{Rate of output of species}\\ \text{i from differential element}\end{bmatrix} + \begin{bmatrix}\text{Rate of species i in by}\\ \text{dispersion}\end{bmatrix} - \begin{bmatrix}\text{Rate of species i out by}\\ \text{dispersion}\end{bmatrix} - \begin{bmatrix}\text{Rate of species i out by}\\ \text{exchange wit emulsion phase}\end{bmatrix} + \begin{bmatrix}\text{Rate of deplection of species i}\\ \text{by chemical reaction}\end{bmatrix} \quad (9)$$

$$\begin{bmatrix}\text{Rate of accumulation}\\ \text{of species i}\end{bmatrix} = \frac{\partial}{\partial t}\left(A_c \Delta h. C_{ci}\right).\sigma \quad (10)$$

$$\begin{bmatrix}\text{Rate of input of species}\\ \text{i into differential}\\ \text{elment}\end{bmatrix} = v_b. A_c. \sigma. C_{ci,b} \quad (11)$$

$$\begin{bmatrix}\text{Rate of output of species}\\ \text{i from differential element}\end{bmatrix} = v_b.A_c.\sigma.(C_{ci,b} + \Delta C_{ci,b}) \quad (12)$$

$$\begin{bmatrix}\text{Rate of species i in by}\\ \text{dispersion}\end{bmatrix} = D_{ci,b}A_c.\sigma\frac{d}{dh}(C_{ci,b}) \quad (13)$$

$$\begin{bmatrix}\text{Rate of species i out by}\\ \text{dispersion}\end{bmatrix} = D_{ci,b}A_c.\sigma\frac{d}{dh}(C_{ci,b} + \Delta C_{ci,b}) \quad (14)$$

$$\begin{bmatrix}\text{Rate of species i out by}\\ \text{exchange wit emulsion phase}\end{bmatrix} = A_c.K_a(C_{ci,b} - C_{ci,b}).\Delta h(\sigma) \quad (15)$$

$$\begin{bmatrix}\text{Rate of deplection of species i}\\ \text{by chemical reaction}\end{bmatrix} = A_c\sigma.\Delta h(r_{c,b}) \quad (16)$$

Substituting (10) to (16) into (9):

$$\frac{\partial}{\partial t}(A_c\sigma.\Delta h.C_{ci,b}) = v_b.A_c\sigma.C_{ci,b} - v_bA_c\sigma.(C_{ci,b} + \Delta C_{ci,b}) + D_{i,b}A_c\sigma.\frac{d}{dh}(C_{ci,b}) \ldots -$$
$$D_{ci,b}A_c\sigma.\frac{d}{dh}(C_{ci,b} + \Delta C_{ci,b}) - A_c\sigma K_a(C_{ci,b} - C_{ci,b}).\Delta h - A_c\sigma.\Delta h(r_{c,b}) \quad (17)$$

$$A_c\sigma.\Delta h\frac{\partial}{\partial t}(C_{ci,b}) = -v_b.A_c\sigma.\Delta C_{ci,b} - D_{ci,b}A_c\sigma.\frac{d}{dh}(\Delta C_{ci,b}) - A_c\sigma K_a(C_{ci,b} - C_{ci,b}).\Delta h - A_c\sigma.\Delta h(r_{c,b}) \quad (18)$$

Dividing (10) by $A_c\sigma.\Delta h$ and taking limit as $\Delta h \to 0$:

$$\frac{\partial C_{ci,b}}{\partial t} = -v_b.\frac{dC_{ci,b}}{dh} - D_{ci,b}.\frac{d^2C_{ci,b}}{dh^2} - K_a(C_{ci,b} - C_{ci,b}) - (r_{c,b}) \quad (19)$$

Assuming steady state ($\frac{\partial C_{ci,b}}{\partial t} = 0$), and negligible axial dispersion ($\frac{d^2C_{ci,b}}{dh^2} = 0$), (11) gives:

$$\frac{dC_{ci,b}}{dh} = -\frac{1}{v_b}[K_a(C_{ci,b} - C_{ci,e}) - (r_{c,b})] \quad (20)$$

where:
A_c = carbonator cross-sectional area (m^2)
σ = volume fraction of bubbles
$C_{ci,b}$ = concentration of species i in the bubble phase ($kmol.m^{-3}$)
$C_{ci,e}$ = concentration of species i in the emulsion phase ($kmol.m^{-3}$)
v_b = bubble rise velocity
K_a = interchange gas transfer coefficient between the phases
$D_{ci,b}$ = dispersion coefficient in the bubble phase.

International Journal of Engineering and Advanced Technology Studies,14 (1),41-63,2026
Print ISSN: 2053-5783(Print)
Online ISSN: 2053-5791(online)
Website: https://www.eajournals.org/
Publication of the European Centre for Research Training and Development -UK

Concentration gradient Model for the Carbonator Emulsion Phase

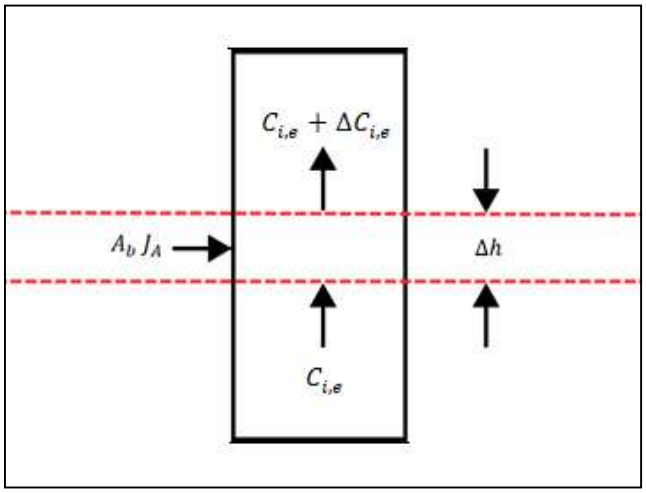

Fig. 2: Differential section of the Emulsion Phase Region

The material balance for the emulsion phase can be derived as follows from the principle of conservation of mass:

$$\left[\begin{matrix}\text{Rate of accumulation}\\ \text{of species i}\end{matrix}\right] = \left[\begin{matrix}\text{Rate of input of species}\\ \text{i into differential}\\ \text{elment}\end{matrix}\right] - \left[\begin{matrix}\text{Rate of output of species}\\ \text{i from differential element}\end{matrix}\right] + \left[\begin{matrix}\text{Rate of species i in by}\\ \text{dispersion}\end{matrix}\right] - \left[\begin{matrix}\text{Rate of species i out by}\\ \text{dispersion}\end{matrix}\right] + \left[\begin{matrix}\text{Rate of species i in by}\\ \text{exchange wit bubble phase}\end{matrix}\right] + \left[\begin{matrix}\text{Rate of generation of species i}\\ \text{by chemical reaction}\end{matrix}\right] \quad (21)$$

$$\left[\begin{matrix}\text{Rate of accumulation}\\ \text{of species i}\end{matrix}\right] = \frac{\partial}{\partial t}(A_c.\Delta h.C_{ci,e}) \quad (22)$$

$$\left[\begin{matrix}\text{Rate of input of species}\\ \text{i into differential}\\ \text{elment}\end{matrix}\right] = v_e.A_c.C_{ci,e} \quad (23)$$

$$\left[\begin{matrix}\text{Rate of output of species}\\ \text{i from differential element}\end{matrix}\right] = v_e A_c.(C_{ci,e} + \Delta C_{ci,e}) \quad (24)$$

$$\left[\begin{matrix}\text{Rate of species i in by}\\ \text{dispersion}\end{matrix}\right] = D_{ci,e}A_c.\frac{d}{dh}(C_{ci,e}) \quad (25)$$

$$\left[\begin{matrix}\text{Rate of species i out by}\\ \text{dispersion}\end{matrix}\right] = D_{ci,e}A_e.\frac{d}{dh}(C_{ci,e} + \Delta C_{ci,e}) \quad (26)$$

$$\begin{bmatrix}\text{Rate of species i in by}\\ \text{exchange wit bubble phase}\end{bmatrix} = A_c K_a (C_{ci,b} - C_{ci,e}).\Delta h \quad (27)$$

$$\begin{bmatrix}\text{Rate of deplection of species i}\\ \text{by chemical reaction}\end{bmatrix} = A_c.\Delta h(r_{c,e}) \quad (28)$$

Substituting into (21)

$$\frac{\partial}{\partial t}(A_c.\Delta h.C_{ci,e}) = v_b.A_c.C_{ci,e} - v_e A_c.(C_{ci,e} + \Delta C_{ci,e}) + D_{i,e}A_c.\frac{d}{dh}(C_{ci,e}) \ldots$$
$$-D_{i,e}A_c.\frac{d}{dh}(C_{ci,e} + \Delta C_{ci,e}) + A_c K_a(C_{ci,b} - C_{ci,e}).\Delta h - A_c.\Delta h(r_{c,e}) \quad (29)$$

$$A_c \Delta h.\frac{\partial C_{ci,e}}{\partial t} = -v_e A_c \Delta C_{ci,e} - D_{ci,e}A_c.\frac{d}{dh}(\Delta C_{ci,e}) + A_c K_a(C_{ci,b} - C_{ci,e}).\Delta h \ldots$$
$$-A_c.\Delta h(r_{c,e}) \quad (30)$$

Dividing through by $A_e.\Delta h$ and taking limit as $\Delta h \to 0$;

$$\frac{\partial C_{ci,e}}{\partial t} = -v_e\frac{dC_{ci,e}}{dh} + D_{ci,e}.\frac{d^2C_{ci,e}}{dh^2} - K_a(C_{ci,b} - C_{ci,e}) + (r_{c,e}) \quad (31)$$

Similarly, assuming steady state ($\frac{\partial C_{i,e}}{\partial t} = 0$) negligible axial dispersion ($\frac{d^2C_{i,e}}{dh^2} = 0$), (31) gives:

$$v_e\delta.\frac{dC_{ci,e}}{dh} = K_a(C_{ci,b} - C_{ci,e}) - (r_{c,e}) \quad (32)$$

$$\frac{dC_{ci,e}}{dh} = \frac{1}{v_e\delta}[K_a(C_{ci,b} - C_{ci,e}) - (r_{c,e})] \quad (33)$$

Where:

A_c = carbonator cross-sectional area (m^2)
$C_{ci,e}$ = concentration of species i in the emulsion phase ($kmol.m^{-3}$)
v_e = emulsion phase velocity (ms^{-1})
$D_{ci,e}$ = dispersion coefficient in the emulsion phase (m^2s^{-1})
$r_{c,e}$ = rate of reaction in the emulsion phase (kgs^{-1})
δ = ratio of fraction of the bed in the emulsion phase to the bubble phase (defined as: $\left(\frac{1-\sigma-\alpha\sigma}{\sigma}\right)$)

Concentration gradient Model for the Regenerator

In the regenerator, solid material is fed into the reactor, where $CaCO_3$ undergoes decomposition to yield pure CaO and CO_2. The modeling of this reactor adheres to a two-region (bubble and emulsion regions) approach utilized in the carbonator model above. However, the gas introduced to induce fluidization is inert. Consequently, the bubble phase will house the pure CO_2 stream, while the decomposition reaction

occurs in the emulsion phase. This signifies that the transfer of CO_2 happens from the emulsion phase to the bubble phase.

Regenerator Bubble Phase

$$\frac{\partial}{\partial t}\left(S_c.\Delta h.C_{ri,b}\right) = u_b.S_c.C_{ri,b} - u_b S_c.\left(C_{ri,b} + \Delta C_{ri,b}\right) + D_{ri,b}S_c.\frac{d}{dh}\left(C_{ri,b}\right) \ldots$$

$$-D_{ri,b}S_c.\frac{d}{dh}\left(C_{ri,b} + \Delta C_{ri,b}\right) + S_c J_A.\Delta h + S_b.\Delta h(r_{r,b}) \quad (34)$$

$$\frac{\partial C_{ri,b}}{\partial t} = -u_b.\frac{dC_{ri,b}}{dh} - D_{ri,b}.\frac{d^2C_{ri,b}}{dh^2} + K_e\left(C_{ri,e} - C_{ri,b}\right) + (r_{r,b}) \quad (35)$$

Assuming steady state ($\frac{\partial C_{ri,b}}{\partial t} = 0$), and negligible axial dispersion ($\frac{d^2C_{ri,b}}{dh^2} = 0$):

$$\frac{dC_{ri,b}}{dh} = \frac{1}{u_b}\left[K_e\left(C_{ri,e} - C_{ri,b}\right) + (r_{r,b})\right] \quad (36)$$

Where:
S_c= regenerator cross-sectional area (m^2)
$C_{ri,b}$ = concentration of species i in the bubble phase in regenerator ($kmol.m^{-3}$)
$C_{ri,e}$ = concentration of species i in the emulsion phase in regenerator ($kmol.m^{-3}$)
u_b = gas velocity in the bubble phase in the regenerator
K_e = interchange gas coefficient between phases
$D_{ri,b}$ = dispersion coefficient in the bubble phase.

Regenerator Emulsion Phase

$$\frac{\partial C_{ri,e}}{\partial t} = -u_e\frac{dC_{ri,e}}{dh} + D_{ri,e}.\frac{d^2C_{ri,e}}{dh^2} - K_e\left(C_{ri,e} - C_{ri,b}\right) + (r_{r,e}) \quad (37)$$

Similarly, assuming steady state ($\frac{\partial C_{ri,e}}{\partial t} = 0$) negligible axial dispersion ($\frac{d^2C_{ri,e}}{dh^2} = 0$), (37) gives:

$$u_e\frac{dC_{ri,e}}{dh} = -K_e\left(C_{ri,e} - C_{ri,b}\right) + (r_{r,e}) \quad (38)$$

$$\frac{dC_{ri,e}}{dh} = \frac{1}{u_e\delta}\left[-K_e\left(C_{ri,e} - C_{ri,b}\right) + (r_{r,e})\right] \quad (39)$$

Where:
u_e = emulsion phase velocity (ms^{-1})
$D_{ri,e}$ = dispersion coefficient in the emulsion phase (m^2s^{-1})
$r_{r,e}$ = rate of reaction in the emulsion phase (kgs^{-1}).

International Journal of Engineering and Advanced Technology Studies,14 (1),41-63,2026
Print ISSN: 2053-5783(Print)
Online ISSN: 2053-5791(online)
Website: https://www.eajournals.org/
Publication of the European Centre for Research Training and Development -UK

RESULTS AND DISCUSSION

Impact of Carbonator Height of Concentration of CO_2

In Figure 3, the concentration profile of CO_2 with respect to carbonator height is presented. The data reveals a distinct trend in which the CO_2 concentration in the flue gas stream decreases noticeably as the height of the carbonator increases within the range of 0 to 5 meters. Specifically, the CO_2 concentration dropped from 71.8 mol/m³ to 8.7 mol/m³ along this height range.

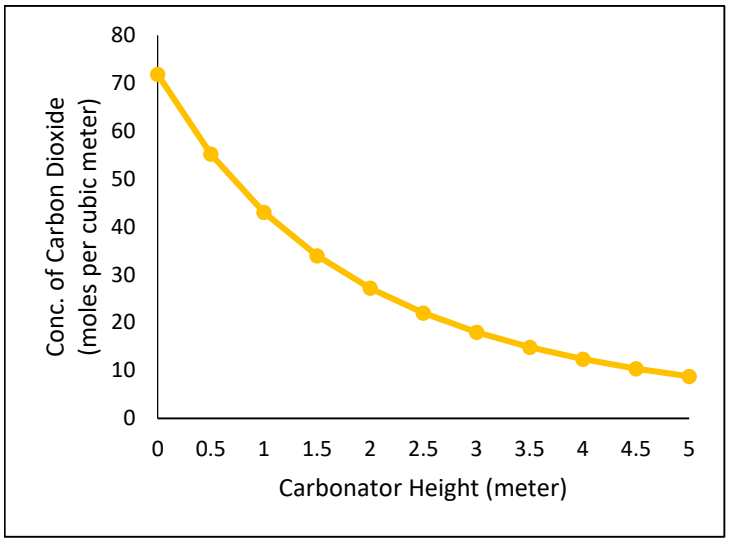

Fig 3: Effect of Carbonator Height on the CO_2 Concentration

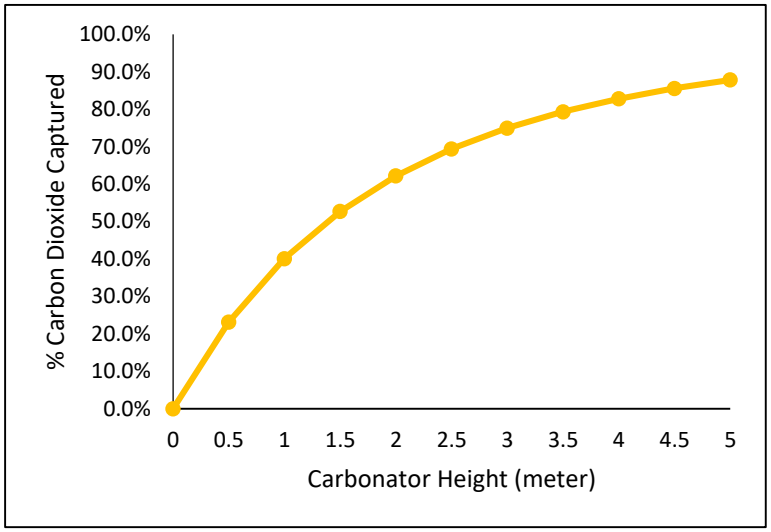

Fig 4: Percentage of Carbon Dioxide Captured in the Carbonator

Figure 4 provides an illustration of the percentage of CO_2 captured from the flue gas by the CaO-sorbent material within the carbonator. By examining this figure in with respect the exit concentration of CO_2 as depicted in Figure 3, it can be inferred that the CaO-sorbent captures approximately 87.8% of the CO_2 from the flue gas.

International Journal of Engineering and Advanced Technology Studies,14 (1),41-63,2026
Print ISSN: 2053-5783(Print)
Online ISSN: 2053-5791(online)
Website: https://www.eajournals.org/
Publication of the European Centre for Research Training and Development -UK

Impact of Regenerator Height of Concentration of CO_2

In Figure 5, presents the concentration profile of CO_2 with respect to regenerator height. The data illustrates a prominent trend wherein the CO_2 concentration within the regenerator experiences a marked increase as the reactor's height advances from 0 to 5 meters. Noticeably, the CO_2 concentration increased from 0 mol/m³ to 44.4 mol/m³ along this height range.

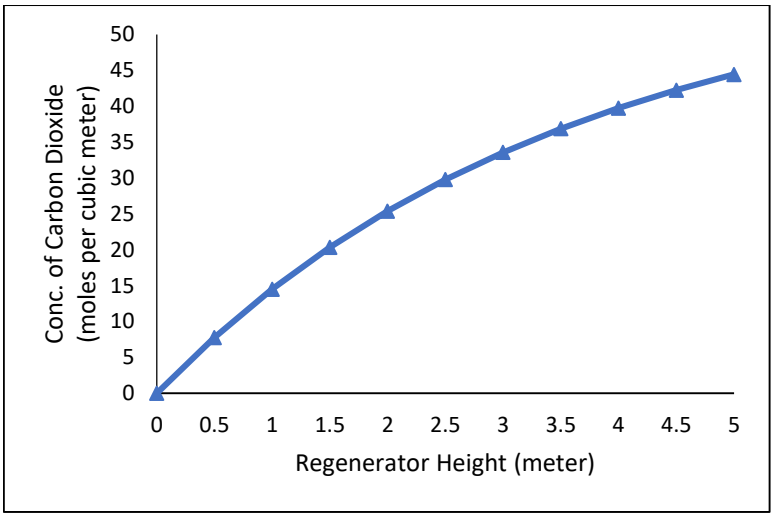

Fig 5: Effect of Regenerator Height on the CO_2 Concentration

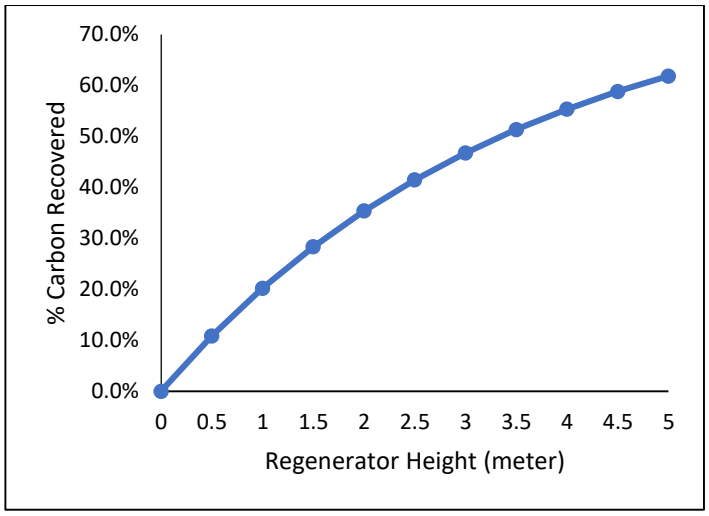

Fig 6: Percentage of Carbon Dioxide Recovered in the Regenerator

Figure 6 provides a visual representation of the percentage of CO_2 recovered through the decomposition of $CaCO_3$ within the regenerator. By examining this figure in with respect to the concentration profile of CO_2 as depicted in Figure 5, it becomes apparent that the $CaCO_3$ decomposition process produced 61.8% of the concentrated CO_2 in the regenerator.

Impact of Carbonation Temperature on Concentration of CO_2

Figure 7 presents an analysis of the impact of varying carbonation temperatures on the concentration of CO_2 within the flue gas along the height of the carbonator. The graphical representation illustrates a clear trend: as the temperature was increased, the CO_2 concentration decreased. Notably, at a temperature of 600°C, the CO_2 concentration dropped from 71.8 mol/m3 to absolute zero. This significant result implied that at 600°C, the carbonator captured 100% of the CO_2 present in the flue gas.

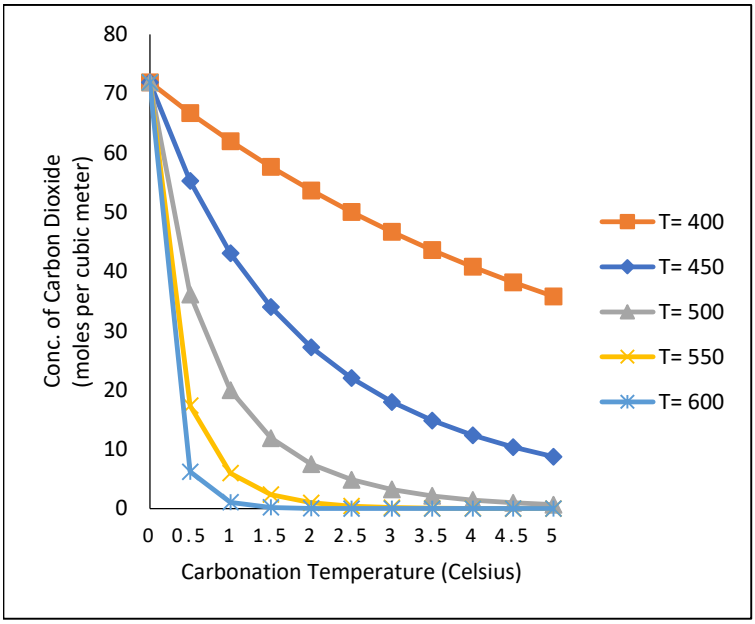

Fig 7: Effect of Carbonation Temperature on the CO_2 concentration

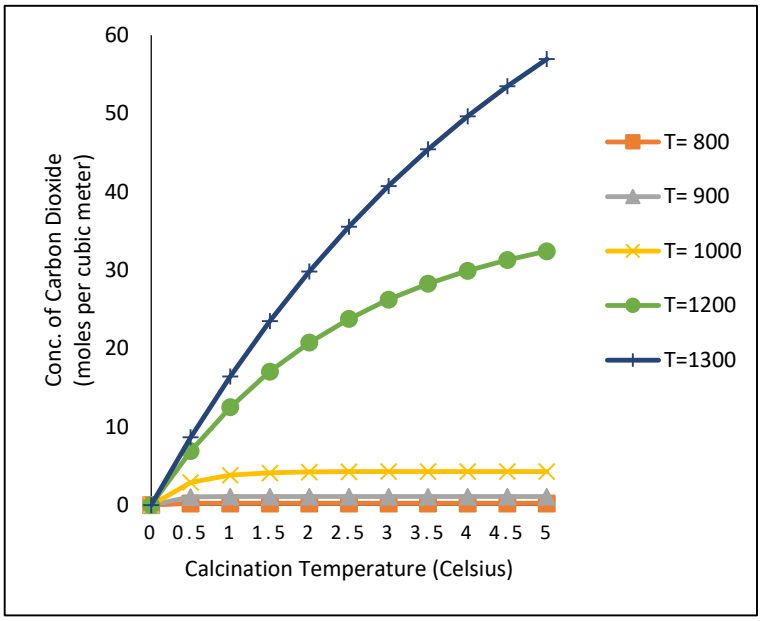

Fig 8: Effect of Calcination Temperature on the CO_2 Concentration

Figure 8 presents a graphical illustration of the impact of varying calcination temperatures on the concentration of CO_2recovered along the height of the regenerator. It was observed that as the temperature was increased, the CO_2 concentration increased significantly. Notably, at a temperature of 1300°C, the CO_2 concentration increased from $0 - 57\ mol/m^3$. This significant increase implied that at the calcination temperature of1300°C, the regenerator recovered79.4% of the CO_2.

The Impact of Residence Time on CO_2 Concentration

The residence time in a reactor is a crucial parameter that can significantly affect the performance of the calcium looping process. Residence time refers to the amount of time that the particles spend inside the reactor. Residence time directly influences the extent to which reactions can occur within the reactor. A longer residence time allows more contact between reactants, which can lead to increased conversion and improved performance. Conversely, a shorter residence time may result in incomplete reactions and lower yields. Prolonged residence time can increase the risk of particle attrition in the carbonator and regenerator. This can affect the physical properties of the particles. Figure 9 presents an effect of varying residence time on the concentration of CO_2 in the flue gas along the height of the carbonator. From the trend it was observed that as the residence time was increased there was slight increase in the concentration of CO_2 in the flue gas at the exit of the carbonator. For best performance, the shorter residence time 10 minutes showed improved capture of CO_2 from the flue gas of 96%.

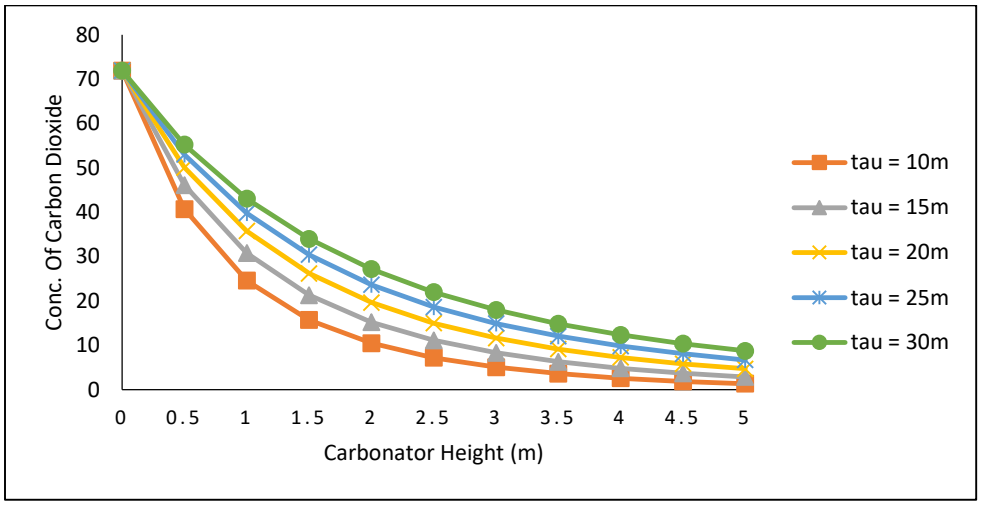

Fig. 9: Effect of Residence time on the CO_2 Concentration in the Carbonator

Figure 10 presents an effect of varying residence time on the concentration of CO_2recovered along the height of the regenerator. From the trend it was observed that as the residence time was increased there was noticeable decrease in the concentration of CO_2 at exit of the regenerator. For best performance, the shorter residence time 10 minutes showed tremendous recovery of the CO_2 gas from 0 to 56.7 mol/m^3.

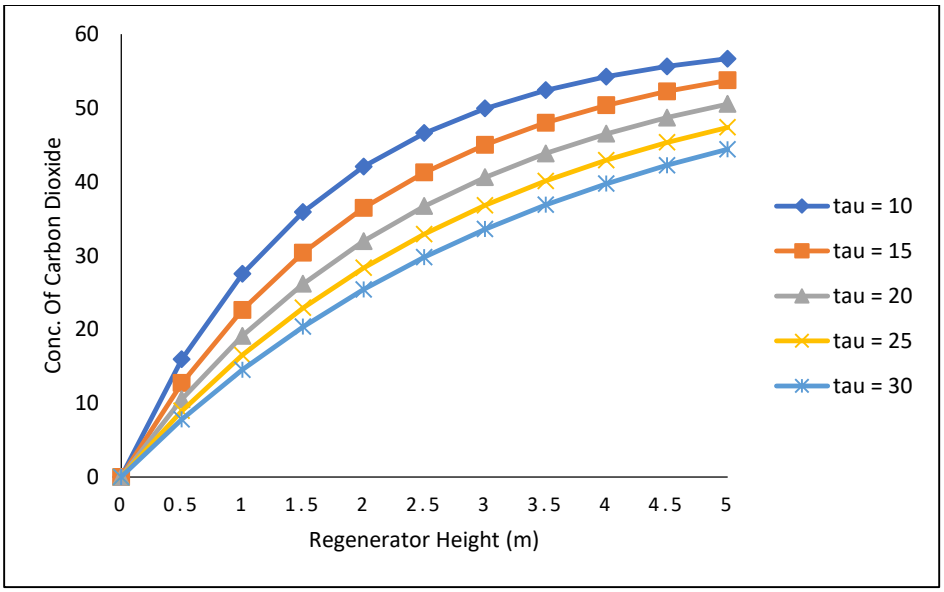

Fig. 10: Effect of Residence time on the CO_2 concentration in the Regenerator

International Journal of Engineering and Advanced Technology Studies,14 (1),41-63,2026
Print ISSN: 2053-5783(Print)
Online ISSN: 2053-5791(online)
Website: https://www.eajournals.org/
Publication of the European Centre for Research Training and Development -UK

Influence of Particle Size of CO_2 Concentration in Carbonator

Figure 4.9 shows the effect of average particle size in the carbonator. It was observed from the trend that as the particle diameter was increased, there was corresponding decrease in the concentration of CO_2 along the reactor height. Notably, for the particle size of 500µm, the concentration of CO_2 in the flue gas dropped from 71.8 to 4.9 mol/m^3.

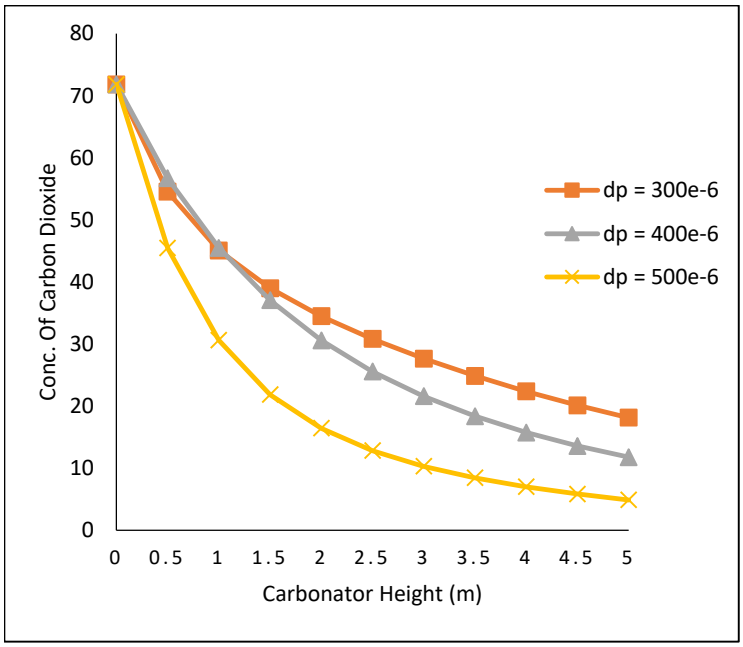

Fig. 4.9: Particle Size Selection for Carbonator

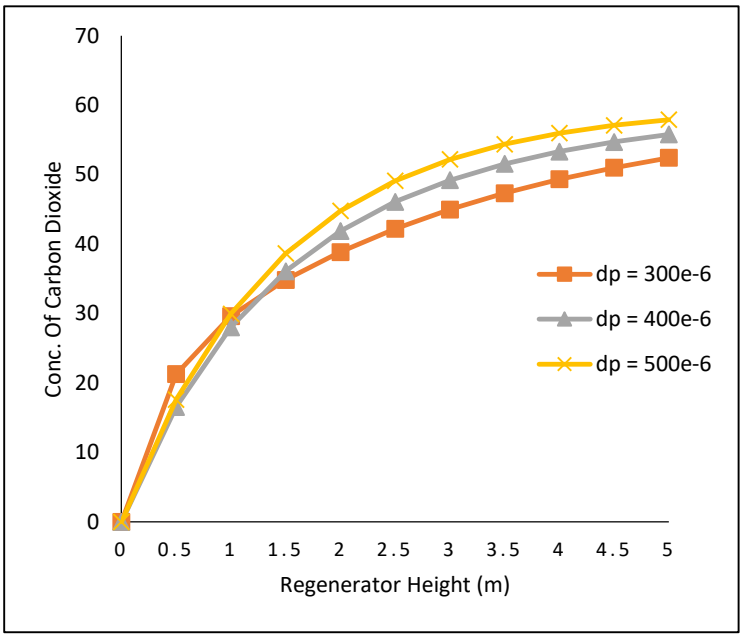

Fig 4.10: Particle Size Selection for Regenerator

Figure 4.10 shows the effect of particle size on the concentration of CO_2 in the regenerator. From the trend, it was evident that as the particle diameter was increased, there was a negligible change in the concentration of CO_2 within the regenerator.

CONCLUSION

Kinetic models for assessment of the calcium looping system behavior are been successfully developed in this work for effective capturing of CO_2 in flue gas emitted from a typical cement producing plant existing in Nigeria power generation unit. The developed models are been achieved via application of the fundamental principles of conservation of mass, energy and momentum. A batch-wise calcium looping system was utilized for this study, and the one-dimensional model for the carbonator and regeneration were developed using the two-phase fluidized bed model by applying the principles of conservation of

mass and energy. Four coupled ordinary differential equations, two for the carbonator and two for the regenerator described the dynamics of the calcium looping process and predicted 87.8% CO_2 captured from the flue gas in the carbonator and 61.9% recovery of concentrated CO_2 in the regenerator. Sensitivity analysis of operational parameters such reactor height, temperature, particle size, and residence time influence capture and recovery of carbon dioxide were conducted using excel suit.

REFERENCE

Ahn, H., Luberti, M., Liu, Z. & Brandani, S. (2013). Process configuration studies of the amine capture process for coal-fired power plants. *International Journal of Greenhouse Gas Control*, 16, 29-40.

Alonso, M., Rodríguez, N., Grasa, G. & Abanades, J. C. (2009). Modelling of a fluidized bed carbonator reactor to capture CO2 from a combustion flue gas. *Chemical Engineering Science*, 64(5), 883-891.

Aouini, I., Ledoux, A., Estel, L. & Mary, S. (2014). Pilot plant studies for CO_2 capture from waste incinerator flue gas using MEA based solvent. Oil & Gas Science and Technology–Revue d'IFP Energies nouvelles, 69(6), 1091-1104.

Benedict U. Ugi, and Fredrick Bekong Ugi (2023). 817M40T Mild Steel Corrosion Remediation in 0.5 M Hydrochloric Acidic Environment Using Alkaloid and Flavonoid Extracts of Salvia Officinalis. *Physical Chemistry Research*, 12(1), 121-133.

Benedict U. U., Faith S. P., V. Bassey, Fredrick Ugi (2022). Expired CYP3A Inhibitor (Ritonavir) as Potential Corrosion Mitigator Of Petroleum Product Trunk Pipeline (20cb-3) in the Oil and Gas Sector. Conference: *Chemical Society of Nigeria South-South Zonal Conference, Workshop and Exhibition* 2022, at: Asaba, Delta State.

Babu, S. P., Shah, B. & Talwalkar, A. (1978). Fluidization correlations for coal gasification materials-minimum fluidization velocity and fluidized bed expansion ratio.

Barla, R. J., Raghuvanshi, S. & Gupta, S. (2022). Process integration for the biodiesel production from biomitigation of flue gases. In Waste and Biodiesel (191-215).

Basile, A., Gugliuzza, A., Iulianelli, A. D.. & Morrone, P. (2011). Membrane technology for carbon dioxide (CO2) capture in power plants. In Advanced membrane Science and Technology for sustainable energy and environmental applications (pp. 113-159). Woodhead Publishing.

Bhatia, S. K. & Perlmutter, D. D. (1983). Effect of the product layer on the kinetics of the CO2-lime reaction. *AIChE Journal*, 29(1), 79-86.

Bhavsar, S., Najera, M., More, A. &Veser, G. (2014). Chemical-looping processes for fuel-flexible combustion and fuel production. In Reactor and Process Design in SustainableEnergy Technology (233-280). Elsevier.

Blamey, J., Anthony, E. J., Wang, J. & Fennell, P. S. (2010). The calcium looping cycle for large scale CO_2 capture. *Progress in Energy and Combustion Science*, 36(2), 260-279.

Blankenship, L. S. & Mokaya, R. (2022). Modulating the porosity of carbons for improved adsorption of hydrogen, carbon dioxide, and methane: A review. *Materials Advances*, 3(4), 1905-1930.

Calix. (n.d.) Our Technology - Innovating for the Earth. https://calix.global/our-technology/.Retrieved 1 October 2023.

Chen, L., Yong, S. Z. & Ghoniem, A. F. (2012). Oxy-fuel combustion of pulverized coal: Characterization, fundamentals, stabilization and CFD modeling. *Progress in Energy and Combustion Science*, 38(2), 156-214.

Dean, C. C., Blamey, J., Florin, N. H., Al-Jeboori, M. J. & Fennell, P. S. (2011). The calcium looping cycle for CO_2 capture from power generation, cement manufacture and hydrogen production. *Chemical Engineering Research and Design*, 89(6), 836-855.

Fang, F., Li, Z. S. & Cai, N. S. (2009). CO_2 capture from flue gases using a fluidized bed reactor with limestone. *Korean Journal of Chemical Engineering*, 26, 1414-1421.

Gilot, P. & Stanmore, B. R. (2005). calcination and carbonation of limestone during thermal cycling for CO_2 sequestration. Fuel processing technology, 86(16), 1707-1743.

Gonzales, V., Krupnick, A. & Dunlap, L. (2020). Carbon capture and storage 101. Resources for the Future.

Hanak, D. P., Anthony, E. J. & Manovic, V. (2015). A review of developments in pilot-plant testing and modelling of calcium looping process for CO 2 capture from power generation systems. *Energy & Environmental Science*, 8(8), 2199-2249.

Igwe C. I., Ugi F.B., Chikwe T. N., Gloria T. T., Ugi B. U., James B. J. (2026) Modeling and Performance Assessment of Produced Water Injection Efficiency in Homogeneous and Heterogeneous Reservoir System as an Enhanced Oil Recovery Approach, International Journal of Petroleum and Gas Engineering Research, 9(1),81-119

Jongpitisub, A., Siemanond, K. & Henni, A. (2015). Simulation of carbon-dioxide-capture process using aqueous ammonia. In Computer Aided Chemical Engineering. 371301-1306. Elsevier.

Ketzer, J. M., Iglesias, R. & Einloft, S. (2017). Reducing Greenhouse Gas Emissions with CO2 Capture and Geological Storage. In Chen, Wei-Yin; Seiner, John; Suzuki, Toshio; Lackner, Maximilian (eds.). Handbook of Climate Change Mitigation. New York: Springer US. 1405–1440. doi:10.1007/978-1-4419-7991-9_37

Kunii, D. & Levenspiel, O. (1991). Fluidization engineering. Butterworth-Heinemann. London.

Lasheras, A., Ströhle, J., Galloy, A., &Epple, B. (2011). Carbonate looping process simulation using a 1D fluidized bed model for the carbonator. *International Journal of Greenhouse Gas Control*, 5(4), 686-693.

Lisbona, P., Martínez, A. & Romeo, L. M. (2013). Hydrodynamical model and experimental results of a calcium looping cycle for CO_2 capture. *Applied Energy*, 101, 317-322.

John, B. B. (2005). Reaction Kinetics and Reactor Design. Marcel Dekker Inc, 2nd ed., 467. ISBN: 0-8247-77220.

Levenspiel, O. (1999). Chemical Reaction Engineering, 3rd ed. John Wiley & Son's Inc, U.S.A.

Modestus O., Abiola A., Ugi F. B. (2025). School Feeding Program in Nigeria: Ethical Issues. International Journal of Scientific Research and Management, 13(02), 8436-8462. DOI: 10.18535/ijsrm/v13i02.em12

Maparanyanga, T., &Lokhat, D. (2021). Modelling of a calcium-looping fluidized bed reactor system for carbon dioxide removal from flue gas. *International Journal of Low-Carbon Technologies*, 16(3), 691-703.

Masson-Delmotte, V., Zhai, P., Pirani, A., Connors, S. L., Péan, C., Berger, S. & Zhou, B. (2021). Climate change 2021: the physical science basis. Contribution of working group I to the sixth assessment report of the intergovernmental panel on climate change, 2.

Medrano, J. A., Gallucci, F., Boccia, F., Alfano, N. & van Sint Annaland, M. (2017). Determination of the bubble-to-emulsion phase mass transfer coefficient in gas-solid fluidized beds using a non-invasive infra-red technique. *Chemical Engineering Journal*, 325, 404-414.

Mori, S. & Wen, C. Y. (1975). Estimation of bubble diameter in gaseous fluidized beds. *AIChE Journal*, 21(1), 109-115.

Ogolo Doris Bruce, Ehirim Emmanuel O., Goodhead T. O., Ugi Fredrick B. (2026). Modeling and Kinetics of Polypropylene Plastic Wastes Depolymerization System to Propylene in Autoclave Recycling Reactor. *International Journal of Scientific Research and Management (IJSRM)*, 14(3), 67-77. DOI: 10.18535/ijsrm/v14i03.ce01

Perry, R. H. & Green, D. W. (2007). Perry's Chemical Engineering Handbook, 8th ed., McGraw Hill, USA.

Romano, M. C. (2012). Modeling the carbonator of a Ca-looping process for CO2 capture from power plant flue gas. *Chemical Engineering Science*, 69(1), 257-269.

Scaltsoyiannes, A. &Lemonidou, A. (2020). CaCO3 decomposition for calcium-looping applications: Kinetic modeling in a fixed-bed reactor. Chemical Engineering Science: X, 8, 100071.

Schakel, W., Hung, C. R., Tokheim, L. A., Strømman, A. H., Worrell, E. & Ramírez, A. (2018). Impact of fuel selection on the environmental performance of post-combustion calcium looping applied to a cement plant. *Applied Energy*, 210, 75-87.

Shimizu, T., Hirama, T., Hosoda, H., Kitano, K., Inagaki, M. & Tejima, K. (1999). A twin fluid-bed reactor for removal of CO_2 from combustion processes. *Chemical Engineering Research and Design*, 77(1), 62-68.

Shukla, P. R., Skea, J., Slade, R., Al Khourdajie, A., Van Diemen, R., McCollum, D., & Malley, J. (2022). Climate change 2022: Mitigation of climate change. Contribution of working group III to the sixth assessment report of the Intergovernmental Panel on Climate Change, 10, 9781009157926.

Silcox, G. D., Kramlich, J. C. & Pershing, D. W. (1989). A mathematical model for the flash calcination of dispersed calcium carbonate and calcium hydroxide particles. *Industrial & Engineering Chemistry Research*, 28(2), 155-160.

Sammy, T. D., Ehirim, E. O. & Ugi, F. B. (2023). Modeling the Effect of Temperature for Enhanced Oil Recovery (EOR) using Steam Injection Technique. Journal of Newviews in Engineering and Technology. 5(1), 22 – 31.

Ugi, F. B., Ehirim, E. O., Wordu, A. A. and Ugi, B. U. (2023). Modelling, design and kinetics of novel Fred-Ugi environmental wastes converter reactor plant for crude oil distillates, minerals and petrochemical synthesis, *International Journal Environmental Engineering*, 12(2), 159–191.

Ugi F.B., Benedict U. Ugi & Gloria T.Tamunotonye (2025). Design of Mechanically Agitated Fermenter for a Daily Ten Tons Ethanol Production from Cool Feed Biomass. ENP Engineering Science Journal, 5(1), 61-69

Ugi B. U, Bassey V. M., Ashishie P. B., Nandi D. O., and Ugi F. B. (2023) S275JR Mild Steel Corrosion Sites Deactivation in Sodium Sesquicarbonate Heavy Deposits Using Piperaquine as Alternative

Inhibitor. *Portugaliae Electrochimica Acta*, 42,101-114 101 https://doi.org/10.4152/pea.2023420202

UGİ, B. U; OJİ, N. N; UGİ, F. B; UGI, D. U; TAMUNOTONYE, G. T (2026). Corrosion Inhibitor Potential of Tropical Milkweed (Asclepias Curassavica) Plant Leaf Extracts for Reinforced Bars in Chloride Concentrated Environment. J. Appl. Sci. Environ. Manage. 30 (2) 481-490

Ugi B. U., Obeten M. E., Bassey V. M., BoEkom E. J., Omaliko E. C., Ugi F. B., Uwah I. E. (2021). Quantum and Electrochemical Studies of Corrosion Inhibition Impact on Industrial Structural Steel (E410) by Expired Amiloride Drug in 0.5 M Solutions of HCl, H2SO4 and NaHCO3. *Moroccan Journal of Chemistry*, 9(4), 677-696 677

Van den Aarsen, F. G. (1985). Fluidised bed wood gasifier performance and modeling. Ph.D. Dissertation, Twente University Publication, University of Twente, 1985.

Voitic, G., Pichler, B., Basile, A., Iulianelli, A., Malli, K., Bock, S. & Hacker, V. (2018). Hydrogen production. In Fuel Cells and Hydrogen (215-241). Elsevier.

Wordu, A. A; Briggs, M. I . F; Ugi, Fredrick. B; Ikenyiri P (2023). Thermodynamics, Kinetics and Equilibrium Analysis of Sulphur dioxide Oxidation in a Catalytic Reactor. *Scientific Research Journal of Engineering and Computer Science*, 3(3), 42-48

Wattanaphan, P., Sema, T., Idem, R., Liang, Z. & Tontiwachwuthikul, P. (2013). Effects of flue gas composition on carbon steel (1020) corrosion in MEA-based CO_2 capture process. *International Journal of Greenhouse Gas Control*, 19, 340-349.

Winter, F. & Schratzer, B. (2013). Applications of fluidized bed technology in processes other than combustion and gasification. In Fluidized bed technologies for near-zero emission combustion and gasification (1005-1033). Woodhead Publishing.

Ylätalo, J., Ritvanen, J., Arias, B., Tynjälä, T. & Hyppänen, T. (2012). 1-Dimensional modelling and simulation of the calcium looping process. International Journal of Greenhouse Gas Control. 9, 130-135.

Zhao, H. & Zhang, M. (2020). Research progress of CaO-based absorbents prepared from different calcium sources. In IOP Conference Series: Earth and Environmental Science (474(5), 052058). IOP Publishing.